Hybrid spectral precoding/windowing for low-latency OFDM

Tayebeh Taheri, Rickard Nilsson and Jaap van de Beek
Department of Computer Science, Electrical and Space Engineering
Luleå University of Technology,SE97187, Luleå, Sweden
{tayebeh.taheri, rickard.o.nilsson, jaap.vandeBeek}@ltu.se

***Abstract*—In this paper we present a joint precoded and windowed OFDM system. This new hybrid method provides flexibility to suppress the out-of band (OOB) emission in non-contiguous OFDM systems used in cognitive radio. This method also provides the possibility of shortening the cyclic prefix without sacrificing the OOB emission or increasing the additional interference which is the case in low-latency future systems.**

I. Introduction

Orthogonal frequency division multiplexing (OFDM) provides in principle a straightforward flexible way to shape the spectrum. By deactivating subcarriers in the vicinity of adjacent users in systems known as non-contiguous OFDM, this property provides the possibility of using spectrum slots left unused by existing systems, see Figure 1. In systems with very tight latency-requirement, however, residual out-of-band (OOB) emissions need special attention, as was very recently established in [1].

Today's OFDM systems have long symbols and an extension by a cyclic prefix that avoids channel-induced interference. New 5G future applications require low latency, for instance in applications where machines are remotely controlled. A long symbol duration may increase the system's latency beyond what is acceptable. In an effort to reduce latency, a shortening of the basic OFDM symbol is straightforward (fewer subcarriers per Hertz). However, the cyclic prefix length is limited by the channel length and cannot be automatically reduced proportional to the symbol length as shortening the cyclic prefix increases the channel-induced interference [2]. This problem in low latency systems was addressed in [3]. Meanwhile, OFDM systems also suffer from high out-of-band (OOB) emissions potentially leading to severe radiation to adjacent bands. Reducing the symbol length results in higher OOB emission. Hence, there appears to be a trade-off between shortening the OFDM symbols and reducing its OOB emissions.

Several methods have been proposed in the literature to suppress the OOB emission including transmit-windowing [4] [5] and spectral precoding [6]. These methods are proposed and analysed individually by themselves in the literature and little attention is given to the effect of symbol shortening. A thorough analysis of the interference in a windowed OFDM system is presented in [1].

In this paper we present a new hybrid precoded/windowed OFDM system, particularly suitable in low-latency systems with a short cyclic prefix. This hybrid system provides better flexibility to suppress OOB emission than precoded or windowed systems. We also analyse the interference in such systems that occurs when the length of channel exceeds the cyclic prefix which is likely to be the dominant scenario in low-latency 5G systems.

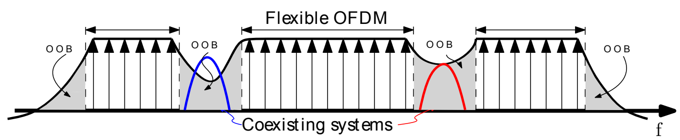

Fig. 1. A non-contiguous OFDM in the presence of coexisting systems. OOB interferes with coexisting systems. Vertical arrows represent used subcarriers. Gray regions show the OOB caused by the OFDM system.

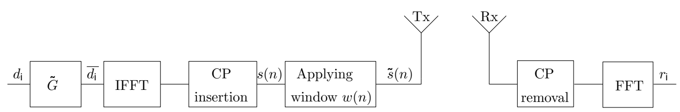

Fig. 2. Hybrid (precoded/windowed) OFDM system block diagram.

After formulating our system model in Section II, we present the hybrid system in Section III. In Section IV we analyse the spectral performance of the hybrid system and compare it with windowing and precoding systems' spectrum. In Section V we investigate different types of interference. Based on analysis in Section IV and V, we discuss the performance for different cyclic prefix lengths and suggest a strategy to select a proper method in different regimes in Section VI.

II. Hybrid system model: precoding and windowing

We first describe a signal model that jointly incorporates two means to reduce OOB power emission: transmit windowing and spectral precoding. We adopt a discrete time OFDM model for the system in Figure 2 and write the transmitted signal as

$$\tilde{s}(n) = \sum_i \tilde{s}_i(n - i(N+L)), \tag{1}$$

where $N+L$ is the length of the OFDM symbol interval, N is the useful part of the OFDM symbol, L is the length of the cyclic prefix and $\tilde{s}_i(n)$ is the ith windowed OFDM symbol,

$$\tilde{s}_i(n) = s_i(n)w(n), \quad -L+1 \le n \le N+W. \tag{2}$$

Here, W is the length of cyclic suffix, $w(n)$ is a window shape chosen as

$$w(n) = \begin{cases} \alpha_{n+L} & n = -L+1, ..., -L+W \\ 1 & n = -L+W+1, ..., N \\ \beta_{n-N} & n = N+1, ..., N+W. \end{cases} \tag{3}$$

978-1-5090-5932-4/17/$31.00 ©2017 IEEE

where α_n and β_n are real-valued and $0\leqslant \alpha_n,\beta_n \leqslant 1$. The signal $s_i(n)$ in (2) represents the OFDM symbol

$$s_i(n) = \sum_k \bar{d}_{i,k} e^{j2\pi \frac{k}{N} n}, \quad -L+1 \leq n \leq N+W \qquad (4)$$

and $s_i(n)$=0 for other values of n. In (4), $\{k_1, k_2, ..., k_K\}$ is the set of subcarrier indices. The OFDM symbol (1) includes a cyclic prefix of length L and a cyclic suffix (CS) of length W. The first and the last W samples of consecutive OFDM symbols overlap and are shaped by the window $w(n)$.

Next to the windowing operation in (2) as one means to control the signal's spectrum, a second means is *precoding*. We incorporate this pre-FFT operation by denoting the vector $\bar{\mathbf{d}}_i = [\bar{d}_{i,1}, \bar{d}_{i,2}, ..., \bar{d}_{i,K}]^T$ as the weighted data symbol, see Figure 2,

$$\bar{\mathbf{d}}_i = \tilde{\mathbf{G}} \mathbf{d}_i, \qquad (5)$$

where $\tilde{\mathbf{G}}$ is a $K\times K$ matrix which represents the precoder and $\mathbf{d}_i = [d_{i,1}, d_{i,2}, ..., d_{i,K}]^T$ represents information data taken from a symbol constellation. Hence, we have two means to control the spectrum: by choice of α and β and by choice of $\tilde{\mathbf{G}}$. Both means come at a price: interference at the receiver. In particular, in the next section we will present a precoder $\tilde{\mathbf{G}}$ that is optimally adapted to the choice of α and β.

We transmit $\tilde{s}(n)$ over a dispersive channel with impulse response $h(n)$ of length H. We are interested in the interference in hybrid precoded-windowed OFDM systems that occurs when the length of $h(n)$ exceeds the cyclic prefix, $H{-}1{>}L$, which is likely to be the dominant scenario in low-latency 5G systems. Our analysis is first based on the interference occurring in one OFDM symbol, as a result of one particular channel impulse response. Later, in our simulations, we evaluate the average interference in the OFDM signal (1).

We continue the approach in [1] and write the received symbol vector after the receiver FFT in precoded windowed OFDM as, see Figure 2,

$$\mathbf{r}_i = \mathbf{D}\bar{\mathbf{d}}_i + \mathbf{G}_{\text{ICI}}\bar{\mathbf{d}}_i + \mathbf{G}_{\text{ISI}}\bar{\mathbf{d}}_{i-1} \qquad (6)$$

where $\mathbf{r}_{\text{i}}=[r_{\text{i},1}\dots r_{\text{i},K}]^T$ is a size-$K\times 1$ vector that contains the received data, where $\mathbf{D}$=diag($\mathbf{Fh}$)=$\mathbf{FHF}^H$ and $\mathbf{h}=[h_1\dots h_H, 0, 0, \dots, 0]$, $\mathbf{F}$ is the $K\times K$ DFT-matrix with entries $[\mathbf{F}]_{xy} = \frac{1}{\sqrt{K}} e^{-2j\pi\frac{xy}{K}}$, ($\mathbf{F}^H$ is the inverse DFT matrix) and $\mathbf{H}$ is the circular channel convolution matrix. The appearance of the cyclic prefix and suffix causes the matrix $\mathbf{D}$ to be diagonal. We can express the matrices $\mathbf{G}_{\text{ISI}}$ and $\mathbf{G}_{\text{ICI}}$ with associated time-domain matrices $\mathbf{H}_{\text{ISI}}$ and $\mathbf{H}_{\text{ICI}}$, presented in detail in [1], as $\mathbf{G}_{\text{ISI}} = \mathbf{F}\mathbf{H}_{\text{ISI}}\mathbf{F}^H$ and $\mathbf{G}_{\text{ICI}} = -\mathbf{F}\mathbf{H}_{\text{ICI}}\mathbf{F}^H$, where $\mathbf{H}_{\text{ISI}}$ and $\mathbf{H}_{\text{ICI}}$ are undesired channel contributions to ISI and ICI respectively. By substituting (5) in (6) we rewrite the received signal as

$$\mathbf{r}_i = \mathbf{D}\tilde{\mathbf{G}}\mathbf{d}_i + \mathbf{G}_{\text{ICI}}\tilde{\mathbf{G}}\mathbf{d}_i + \mathbf{G}_{\text{ISI}}\tilde{\mathbf{G}}\mathbf{d}_{i-1}. \qquad (7)$$

The first term in (7) contains the desired signal and the additive interference caused by the precoder and the second and third terms are ICI and ISI due to the channel, respectively. Here we note that if there is no precoding, $\tilde{\mathbf{G}} = \mathbf{I}$, the first term in (7) reduces to the orthogonal desired signal without any additive interference. Moreover, in case of sufficiently long cyclic prefix the last two interference terms in (7) disappear. In Section V we will discuss each term of (7) in more detail.

In the following sections, we first design a suitable precoder $\tilde{\mathbf{G}}$, we then analyse the spectrum of the hybrid system, and finally, using (7) we analyse different types of interferences in the hybrid system in detail.

III. Design of the Precoder Given a Certain Window

Instead of transmitting the plain constellation points, $\mathbf{d}_i$, the precoder linearly modifies the data as in (5). To calculate matrix $\tilde{\mathbf{G}}$ which provides such modification to $\mathbf{d}_i$, we rewrite the transmitted symbol (2) as a multiplex of windowed modulated subcarriers $\tilde{p}_k(n)$,

$$\tilde{s}_i(n) = \sum_k \bar{d}_{i,k}\tilde{p}_k(n), \qquad (8)$$

where $\tilde{p}_k(n) = e^{j2\pi\frac{k}{N}n} w(n)$ is the kth windowed modulated subcarrier. By applying the Fourier transform to (8),

$$\tilde{S}_i(f) = \sum_k \bar{d}_{i,k}\tilde{a}_k(f) = \tilde{\mathbf{a}}^T(f)\bar{\mathbf{d}}_i, \qquad (9)$$

where $\tilde{S}(f) \stackrel{\text{def}}{=} F\{\tilde{s}(n)\}$, $\tilde{a_k}(f) \stackrel{\text{def}}{=} F\{\tilde{p_k}(n)\}$, $F\{.\}$ indicates the *discrete-time* Fourier transform, and $\tilde{\mathbf{a}}(f) = [\tilde{a}_1(f), \tilde{a}_2(f), ..., \tilde{a}_K(f)]^T$. The power spectrum $P(f)$ of (1) is then

$$P(f) = \frac{1}{T}E\{|\tilde{S}_i(f)|\}^2 = \frac{1}{T}\|\tilde{\mathbf{G}}^T\tilde{\mathbf{a}}(f)\|_2^2, \qquad (10)$$

where the expectation $E\{\cdot\}$ is over all possible symbols. Here, we assume that the data are uncorrelated, $E\{\mathbf{d}_i\mathbf{d}_i^H\}$=$\mathbf{I}_K$ and $E\{\mathbf{d}_i\mathbf{d}_j^H\}$=$\mathbf{0}_K$ if $i{\neq}j$. Note that (8)-(10) is different from [6] in that our model is a discrete time model, hence, $\tilde{\mathbf{a}}(f)$ is the discrete time Fourier transform with a normalized frequency. A more conceptual and important difference of (8)-(10) with [6], however, is that the window shape $w(n)$ is now explicitly taken into account.

Following [6], we force the power spectrum $P(f)$ to be zero at M specific frequencies of $f_0, f_1, ..., f_{M-1}$ which in turn leads to $\tilde{\mathbf{a}}(f_0) = 0$, $\tilde{\mathbf{a}}(f_1) = 0$, ... and $\tilde{\mathbf{a}}(f_{M-1}) = 0$. We hope that this requirement will also have a suppressing effect on other frequencies than $\{f_0, ..., f_{M-1}\}$. Using (9) we find

$$\tilde{\mathbf{A}}\bar{\mathbf{d}}_i = 0, \qquad (11)$$

where

$$\tilde{\mathbf{A}} = \begin{bmatrix} \tilde{a}_1(f_0) & \tilde{a}_2(f_0) & \dots & \tilde{a}_K(f_0) \\ \tilde{a}_1(f_1) & \tilde{a}_2(f_1) & \dots & \tilde{a}_K(f_1) \\ \vdots & \vdots & & \vdots \\ \tilde{a}_1(f_{M-1}) & \tilde{a}_2(f_{M-1}) & \dots & \tilde{a}_K(f_{M-1}) \end{bmatrix} \qquad (12)$$

is a $K\times M$ matrix dependent on the window shape $w(n)$ and completely known. The solution to (11) is the precoder of the well-known form

$$\tilde{\mathbf{G}} = \mathbf{I} - \tilde{\mathbf{A}}^H(\tilde{\mathbf{A}}\tilde{\mathbf{A}}^H)^{-1}\tilde{\mathbf{A}}. \qquad (13)$$

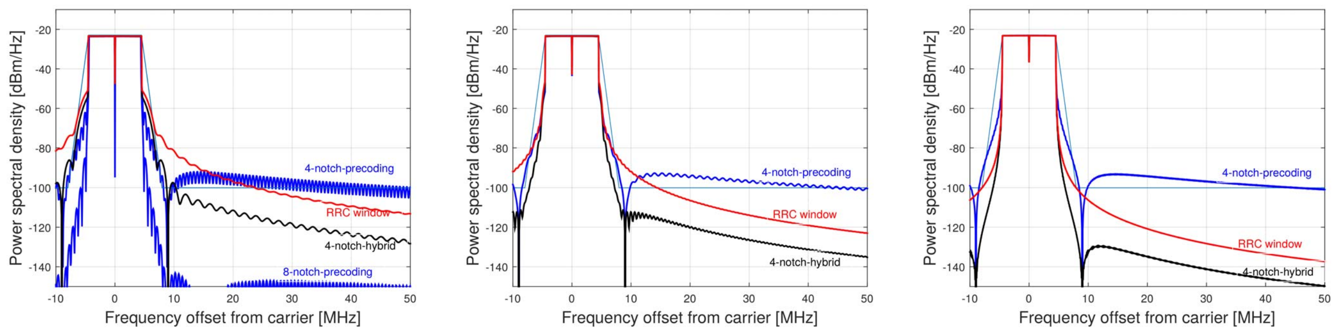

(a) L=0.26μs (b) L=0.78μs (c) L=3.9μs

Fig. 3. Power spectrum for RRC-windowed ($W = L$), 4-notch-precoded (notches at $\pm$8.9 and $\pm$9 MHz) and corresponding 4-notch-hybrid OFDM system in a fully used spectrum for the cyclic prefix length of a) L=0.26μs, b) L=0.78μs, c) L=3.9μs. An 8-notch-precoded system (notches at $\pm$8.9, $\pm$9, $\pm$14.9 and $\pm$15 MHz) is also depicted in (a).

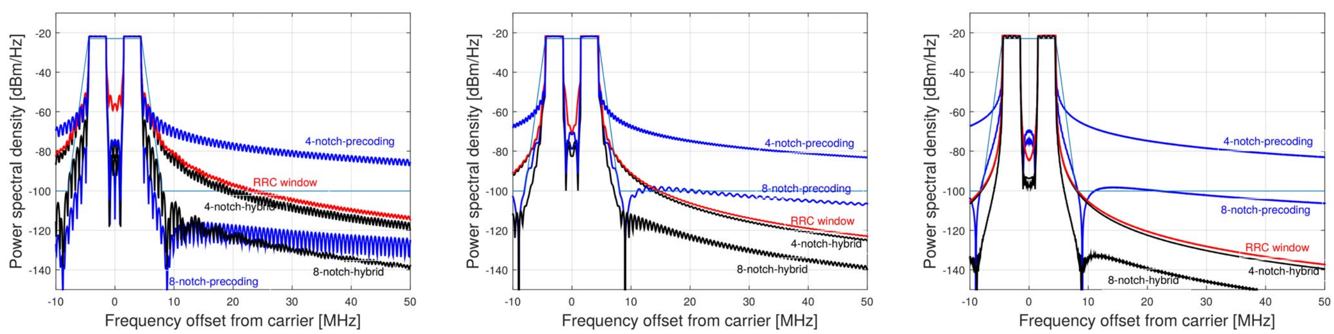

(a) L=0.26μs (b) L=0.78μs (c) L=3.9μs

Fig. 4. Power spectrum for RRC-windowed ($W = L$), 4-notch-precoded (notches at $\pm$8.9 and $\pm$9 MHz), 8-notch-precoded (notches at $\pm$1, $\pm$1.1, $\pm$8.9 and $\pm$9 MHz) and corresponding 4 and 8-notch-hybrid OFDM system in a partially used spectrum for the cyclic prefix length of a) L=0.26μs, b) L=0.78μs, c) L=3.9μs.

Precoder (13) is a new precoder in the sense that it is particularly designed for the window $w(n)$. The precoder in [6] is a special case of (13) with the rectangular window ($W = 0$ in (3)) and windowing is a hybrid system with $\tilde{\mathbf{G}} = \mathbf{I}$.

IV. Spectral analysis

As a first step in the analysis of the new precoder (13), we plot the spectrum (10) for an LTE system with 10MHz channel bandwidth, 600 sub-carriers, of symbols of length 66.7μs and the cyclic prefix length 4.7μs. In figures 3 and 4 the spectral mask reflects future requirements for an ultra-robust system which is 17 dB stricter than the spectral mask defined by LTE standards [7]. The spectra in Figures 3 and 4 show the power spectrum (10) for a very high sample rate, hence, our discrete-time signal analysis approaches that of the continuous time equivalent of (1).

We explore the OOB emission suppression of our system in two scenarios. In a first scenario we assess the classical OOB emission of a fully loaded OFDM system. Figure 3 shows the power spectrum of a 4-notch-precoded system, a windowed OFDM system (with root raised-cosine (RRC) window [8], where the whole cyclic prefix is used for windowing) and the corresponding 4-notch-hybrid system (which is the combination of two other systems) for three different cyclic prefix lengths. We see that in all three cases the hybrid system improves the OOB emission suppression compared to the pure windowing and the pure precoding.

In a second scenario we suppress OOB emission in a partially loaded OFDM spectrum. Here we notch out one third of the spectrum located in the center of the spectrum. In this scenario the hybrid system exploits the properties of both precoding and windowing where needed. For example a 4-notch-hybrid system where the notches are in inner side (cancelled subcarrier region) exploits the property of precoding to suppress the OOB emission in inner side. This hybrid system also exploits the property of the windowing to suppress the OOB emission in outer side. Figure 4 shows that windowing method does not have considerable effect on OOB emision in inner side even though it suppresses OOB in outer side.

Figure 4 also shows that a 4-notch-precoder whose notches are located in inner side of the spectrum suppresses the OOB in inner side but it does not suppress the OOB in outer side of the spectrum. Combining these two systems (windowing and 4-notch-precoding) leads to a 4-notch-hybrid system which affects OOB in both inner and outer sides of the spectrum.

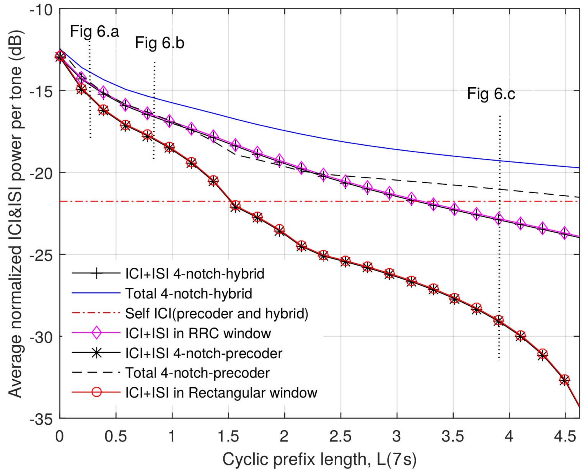

Fig. 5. Average total power of different types of interference in an only RRC-windowed, an only 4-notch-precoded and corresponding 4-notch hybrid system versus cyclic prefix length. The whole cyclic prefix length is used for windowing ($W = L$) and notches are located at ± 8.9 and ± 9 MHz

It is clear that with a higher order precoder, both the precoder and the hybrid system become better in their OOB emission suppression, see the 8-notch-precoding curves and the 8-notch-hybrid curves in Figures 3 and 4. Moreover, with a smoother window (longer cyclic prefix) both hybrid and windowing methods become better.

We conclude that in terms of OOB emission the hybrid system is a better option than the windowing or a precoding system. For a fair comparison, we analyse the interferences caused by the hybrid system.

V. Interference Analysis

We first rewrite (7) as

$$\mathbf{r}_i = \mathbf{D}\mathbf{d}_i + \mathbf{D}(\tilde{\mathbf{G}} - \mathbf{I})\mathbf{d}_i + \mathbf{G}_{\text{ICI}}\tilde{\mathbf{G}}\mathbf{d}_i + \mathbf{G}_{\text{ISI}}\tilde{\mathbf{G}}\mathbf{d}_{i-1}. \quad (14)$$

The first term in (14) is the desired signal, the second term is the additive interference caused by the precoder and the third and fourth terms are ICI and ISI due to the channel, respectively.

A. Self-ICI due to the precoder

We assume that the data is uncorrelated, $E\{\mathbf{d}_i\mathbf{d}_i^H\}=\mathbf{I}_K$ and $E\{\mathbf{d}_i\mathbf{d}_j^H\}=\mathbf{0}_K$ if $i\neq j$. The introduced error by the precoder is

$$\mathbf{e}_i = (\mathbf{I} - \tilde{\mathbf{G}})\mathbf{d}_i = \tilde{\mathbf{A}}^H(\tilde{\mathbf{A}}\tilde{\mathbf{A}}^H)^{-1}\tilde{\mathbf{A}}\mathbf{d}_i. \quad (15)$$

As $(\mathbf{I} - \tilde{\mathbf{G}})$ is a projection matrix, the power of the additive ICI due to the precoder becomes [6]

$$\begin{aligned}\mathbf{P}_{\text{self-ICI, total}} &= \text{Tr}\{E\{\mathbf{e}_i\mathbf{e}_i^H\}\} = \text{Tr}\{(\mathbf{I} - \tilde{\mathbf{G}})(\mathbf{I} - \tilde{\mathbf{G}})^H\} \\ &= \text{Tr}\{\mathbf{I} - \tilde{\mathbf{G}}\} = \text{Rank}\{\mathbf{I} - \tilde{\mathbf{G}}\} = M, \quad (16)\end{aligned}$$

where expectation is performed over all possible data symbols. The rank of the projection matrix is independent of the window, hence, surprisingly, the total ICI due to precoding does not depend on the window. In contrast, the self-ICI power on the kth subcarrier is

$$\mathbf{P}_{\text{self-ICI, k}} = \left[E\{\mathbf{e}_i\mathbf{e}_i^H\}\right]_{kk} = \left[\mathbf{I} - \tilde{\mathbf{G}}\right]_{kk} \quad (17)$$

which does depend on the particular window-choice. In the next section we will evaluate this interference further.

B. ISI and ICI due to the channel for hybrid system

The covariance matrix of the channel-induced ISI-term in (14), $\mathbf{G}_{\text{ISI}}\bar{\mathbf{d}}_{i-1}$, becomes

$$\mathbf{C}_{\text{ISI}} \overset{\text{def}}{=} E\{\mathbf{G}_{\text{ISI}}\bar{\mathbf{d}}_{i-1}\bar{\mathbf{d}}_{i-1}^H{\mathbf{G}_{\text{ISI}}}^H\} = E\{\mathbf{G}_{\text{ISI}}\tilde{\mathbf{G}}{\mathbf{G}_{\text{ISI}}}^H\}, \quad (18)$$

because $E\{\bar{\mathbf{d}}_i\bar{\mathbf{d}}_i^H\} = \tilde{\mathbf{G}}$. Similarly, the covariance matrix of the channel-induced ICI-term in (14), $\mathbf{G}_{\text{ICI}}\bar{\mathbf{d}}_i$, becomes

$$\mathbf{C}_{\text{ICI}} = E\{\mathbf{G}_{\text{ICI}}\tilde{\mathbf{G}}{\mathbf{G}_{\text{ICI}}}^H\}. \quad (19)$$

The diagonal elements of these covariance matrices contain the interference power of the respective subcarrier,

$$\mathbf{P}_{\text{ICI},k} = [\mathbf{C}_{\text{ICI}}]_{kk} \quad \text{and} \quad \mathbf{P}_{\text{ISI},k} = [\mathbf{C}_{\text{ISI}}]_{kk}\,. \quad (20)$$

The total ICI power is the trace of $\mathbf{C}_{\text{ICI}}$, $\text{Tr}\{\mathbf{C}_{\text{ICI}}\}$, using the property $\text{Tr}\{\mathbf{AB}\} = \text{Tr}\{\mathbf{BA}\}$ we find that

$$\mathbf{P}_{\text{ICI,total}} = \text{Tr}\{\mathbf{C}_{\text{ICI}}\} = \text{Tr}\left\{{\mathbf{G}_{\text{ICI}}}^H\mathbf{G}_{\text{ICI}}\tilde{\mathbf{G}}\right\} \quad (21)$$

and similarly, the total ISI power is

$$\mathbf{P}_{\text{ISI,total}} = \text{Tr}\left\{{\mathbf{G}_{\text{ISI}}}^H\mathbf{G}_{\text{ISI}}\tilde{\mathbf{G}}\right\}. \quad (22)$$

Furthermore, it is straightforward to show that ISI, ICI and self-ICI are uncorrelated. Therefore, the total interference power of the system is

$$\mathbf{P}_{\text{total}} = \mathbf{P}_{\text{ISI,total}} + \mathbf{P}_{\text{ICI,total}} + \mathbf{P}_{\text{self-ICI,total}}. \quad (23)$$

As we discussed, in emerging low latency applications the cyclic prefix needs to be as short as possible. Therefore, we investigate the amount of interference that occurs for any cyclic prefix length (up to $4.7\mu s$ used in today's LTE standard). We use the extended typical urban fading channel model (ETU) (introduced in the annex B of [7]) and results from 1000 channel realizations are averaged.

Figure 5 shows the total channel-induced interference, the total self-ICI and the total interference (23) for an RRC-windowed ($W = L$), 4-notch precoder and the corresponding 4-notch hybrid systems for different cyclic prefix lengths in the fully loaded OFDM system introduced in Section IV. For longer cyclic prefixes, the total interference in the hybrid system is dominated by self-interference while for short cyclic prefix lengths, channel-induced interference plays the key role.

The most important conclusion from Figure 5, is that the total interference power in a windowed OFDM system is less than the total interference of a precoded system. Moreover, combining windowing and precoding increases the total interference. Simulations, not shown in this paper, indicate similar interference behaviour for scenario 2 (introduced in Section IV).

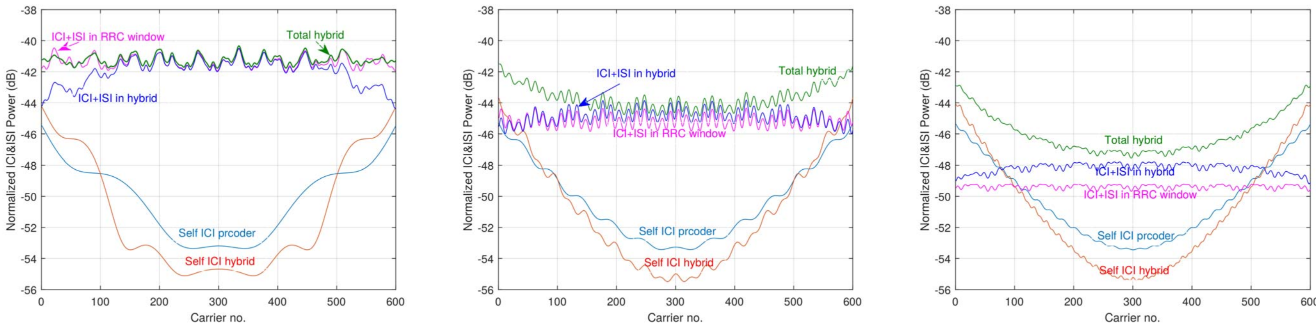

(a) L=0.26μs (b) L=0.78μs (c) L=3.9μs

Fig. 6. Interference power per subcarrier. Cyclic prefix length of a) L=0.26μs, b) L=0.78μs, c) L=3.9μs. The whole cyclic prefix length is used for windowing ($W = L$) and notches are located at $\pm$8.9 and $\pm$9 MHz.

Figure 6 shows the different interference power on each subcarrier for three different cyclic prefix lengths. For a short cyclic prefix the total interference on each subcarrier is dominated by the channel-induced interference and is almost the same as interference in a system without precoding. By increasing the cyclic prefix length, the total interference on middle subcarriers decreases and hence, the total interference power in the system decreases.

VI. Performance Discussion

We now combine our insights from the spectral analysis in Section IV and the interference in Section V. Depending on the length of the cyclic prefix, a different spectral shaping approach is desirable.

For short cyclic prefix regimes precoding or hybrid, depending on the cyclic prefix length, is the best approach to suppress the OOB emission. As we use some part of the cyclic prefix to apply the window, if cyclic prefix is extremely short (less than 0.5μs), there is no possibility of using windowing. So, the only method to suppress the OOB emission effectively is precoding. In such regimes we have to add notches wherever needed (inner and outer sides) until we achieve acceptable OOB emission suppression, see Figures 3a and 4a. Adding notches increases the interference considerably. If the cyclic prefix becomes longer (more than 0.5μs) there is a possibility of using a window. In such regimes, instead of using a high order precoding with high amount of interference, a lower order hybrid system suppress the OOB emission with lower amount of interference, see Figures 3b and 4b.

For long cyclic prefix regimes hybrid or windowing, depending on the scenario, is the best approach to suppress the OOB emission. When the cyclic prefix is long enough to provide the possibility of a smooth window to suppress OOB emission below the mask, there is no reason to use anything else than windowing, see Figure 3c. Finally in the scenario of non-contiguous OFDM, even for a long cyclic prefix, windowing is not a proper method as it cannot suppress the OOB emission in inner side effectively. Here, a 4-notch hybrid system suppresses OOB emission in both inner and outer side perfectly, see Figure 4c.

The above regimes are clearly conceptual: depending on the channel length and system tolerance the notion of a short, or long, cyclic prefix varies.

VII. Conclusion

In this paper we propose a new hybrid precoding/windowing method to suppress the out-of-band (OOB) emission. Our method is useful for cognitive radio systems as it provides the possibility to flexibly and effectively share the spectrum. Simulation results show that in low-latency 5G system where none of windowing or precoding system can suppress the OOB emission efficiently, the hybrid system suppresses OOB emission effectively with low additional interference.

Acknowledgement

Parts of this work were carried out with financial support from the Swedish Research Council, grant nr 2014-5977, which we gratefully acknowledge.

References

[1] T. Taheri, R. Nilsson *et al.*, “Asymmetric transmit-windowing for low-latency and robust OFDM,” in *IEEE International Conference on Global Communications (GLOBECOM 2016), Third International Workshop on Ultra-Reliable and Low-Latency Communications in Wireless Networks (URLLC), Washington DC, USA, 4-8 December 2016*, 2016.

[2] W. Henkel, G. Tauböck, P. Ödling, P. O. Börjesson, and N. Petersson, “The cyclic prefix of OFDM/DMT-an analysis,” in *Broadband Communications, 2002. Access, Transmission, Networking. 2002 International Zurich Seminar on*. IEEE, 2002, pp. 22–1.

[3] J. Lorca, “Cyclic prefix overhead reduction for low-latency wireless communications in OFDM,” in *Vehicular Technology Conference (VTC Spring), 2015 IEEE 81st*. IEEE, 2015, pp. 1–5.

[4] A. Sahin and H. Arslan, “Edge windowing for OFDM based systems,” *Communications Letters, IEEE*, vol. 15, no. 11, pp. 1208–1211, 2011.

[5] E. Guvenkaya, E. Bala, R. Yang, and H. Arslan, “Time-asymmetric and subcarrier-specific pulse shaping in OFDM-based waveforms,” *Vehicular Technology, IEEE Transactions on*, vol. 64, no. 11, pp. 5070–5082, 2015.

[6] J. van de Beek, “Sculpting the multicarrier spectrum: a novel projection precoder,” *IEEE Communications Letters*, vol. 13, no. 12, pp. 881–883, 2009.

[7] *Evolved Universal Terrestrial Radio Access (E-UTRA); Base Station (BS) radio transmission and reception (Release 13)*, 3GPP TSG RAN TS 36.104, v13.0.0., Jan. 2016. [Online]. Available: http://www.3gpp.org/

[8] S. Lmai, A. Bourre, C. Laot, and S. Houcke, “Advantages of pulse-shaping applied to OFDM systems over underwater acoustic channels,” in *Oceans, 2012*. IEEE, 2012, pp. 1–7.